

# Chemical Amplification: Continuous-Flow PCR on a Chip

Martin U. Kopp, Andrew J. de Mello, Andreas Manz\*

A micromachined chemical amplifier was successfully used to perform the polymerase chain reaction (PCR) in continuous flow at high speed. The device is analogous to an electronic amplifier and relies on the movement of sample through thermostated temperature zones on a glass microchip. Input and output of material (DNA) is continuous, and amplification is independent of input concentration. A 20-cycle PCR amplification of a 176–base pair fragment from the DNA gyrase gene of *Neisseria gonorrhoeae* was performed at various flow rates, resulting in total reaction times of 90 seconds to 18.7 minutes.

Electronic amplifiers allow weak signals to be increased by a large constant factor with the same time dependency and virtually no time delay. Although some biochemical systems, such as hormonal signaling, lead to large amplifications, they often do so nonlinearly and with time delays. A true chemical amplifier, which would continuously amplify the concentration of a compound independent of the input concentration, could be extremely useful in analysis and process control. In particular, a capillary-shaped chemical reactor with its inherent low-dispersion characteristics could maintain the shape of analyte peaks injected sequentially, yielding the amplified product in the same volume element. Unlike electronic amplification, additional molecules must be synthesized from building blocks or transformed from precursor species. This process involves both chemical reaction kinetics and diffusion-limited mass transport, and will lead to more significant time delays than those in an electronic amplifier.

This chemical amplifier concept could be applied to a number of known reactions, such as self-activating enzymatic reactions, cyclic electrochemical reactions, and polymerizations. We have focused on PCR (1), which doubles the number of specific DNA molecules during each cycle of melting of the double-stranded DNA (dsDNA), binding of the specific primers to their target sites (annealing), and extending of the primers with the thermostable DNA polymerase (such as Taq). The individual steps are simply performed by heating or cooling the sample to characteristic temperatures: 95°C for dsDNA melting, 50° to 65°C for primer annealing, and 72° to 77°C for primer extension at the optimum enzyme temperature. Conventionally, this process is performed with a programmable instrument that heats and cools a tube,

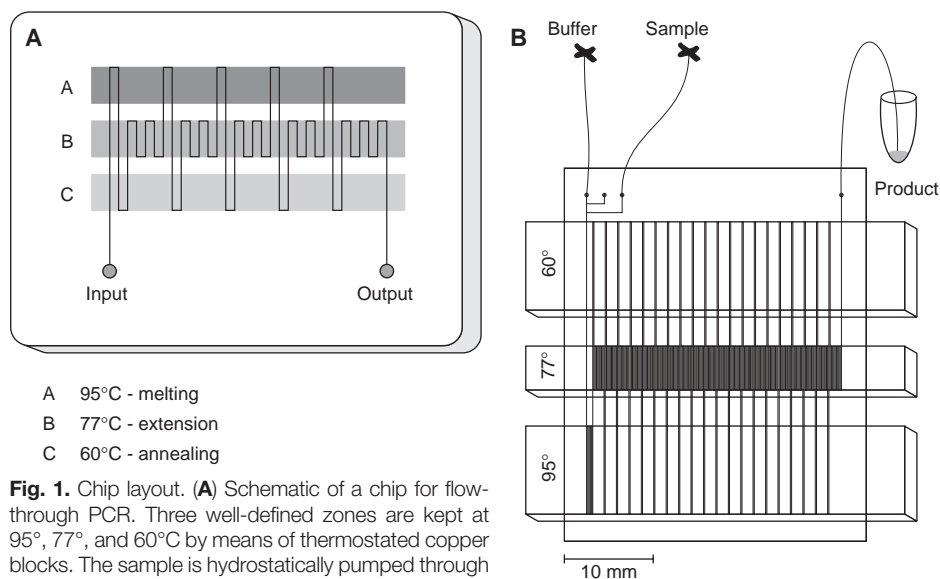
capillary, or slide containing the reagent mixture. The product is then analyzed by an endpoint measurement or directly used for cloning and sequencing.

PCR represents a perfect model reaction for a chemical amplifier. Conventional thermal cyclers are based on batch processes and therefore do not represent a chemical amplifier in the previously described sense. Here, we present a microfabricated device

performing PCR in a continuous flow at high speed. The results demonstrate the concept of a chemical amplifier for DNA.

The speed of thermal cycling is usually instrument limited, except for a commercial system that uses an air stream to heat and cool sealed glass capillaries containing the PCR mixture; this system has demonstrated high thermal cycling speeds and efficient amplification (2). More recently, several groups have reported high cycling speeds for PCR and the ligase chain reaction (LCR) with various designs of micromachined heating chambers (3, 4). Micromachining can be defined as the patterning of silicon and its derivatives to create three-dimensional microstructures. A wide range of microreactors, microcapillary electrophoresis devices, and microcell manipulation devices have been described in recent years (5).

A continuous-flow PCR system can be realized by a time-space conversion in the PCR system—that is, by keeping temperatures constant over time at different locations in the system and moving the sample through the individual temperature zones (Fig. 1A). The time delay for the sample to



- A 95°C - melting
- B 77°C - extension
- C 60°C - annealing

**Fig. 1.** Chip layout. **(A)** Schematic of a chip for flow-through PCR. Three well-defined zones are kept at 95°, 77°, and 60°C by means of thermostated copper blocks. The sample is hydrostatically pumped through a single channel etched into the glass chip. The channel passing through the three temperature zones defines the thermal cycling process. **(B)** Layout of the device used in this study. The device has three inlets on the left side of the device and one outlet to the right. Only two inlets are used: one carrying the sample, the other bringing a constant buffer flow. The whole chip incorporates 20 identical cycles, except that the first one includes a threefold increase in DNA melting time. The chip was fabricated in Corning 0211 glass at the Alberta Microelectronic Centre, Canada. All channels are 40  $\mu\text{m}$  deep and 90  $\mu\text{m}$  wide; the etched glass chip and the cover plate are each 0.55 mm thick. Access to the channels is provided by holes (400  $\mu\text{m}$ ) drilled into the cover plate. Standard fused-silica capillaries (outside diameter 375  $\mu\text{m}$ , inside diameter 100  $\mu\text{m}$ ) are glued with epoxy into the holes of the chip. Virtually no dead volume is introduced by this connection. Two precision syringe pumps (Kloehn 50300, 25  $\mu\text{l}$ ) deliver the PCR sample and the buffer solution onto the chip. The pumps are controlled by a program written in Labview running on a PC. Product is collected at the outlet capillary and then analyzed by slab-gel electrophoresis. The copper blocks are heated by 5-W heating cartridges, and the surface temperature is monitored by a Pt100 thin-film resistor mounted on the surface of the block near the chip contact area. Cooling fins passively cool the two blocks at 77° and 60°C. The temperature controllers are built with standard PID (proportional, integral, and derivative) digital temperature controllers (CAL 3200), power supplies, and switching electronics for the heating cartridges.

Zeneca/SmithKline Beecham Centre for Analytical Sciences, Department of Chemistry, Imperial College of Science, Technology and Medicine, London SW7 2AY, UK.

\*To whom correspondence should be addressed. E-mail: a.manz@ic.ac.uk

reach a new temperature depends only on the times needed to transport the sample into the appropriate temperature zone to heat a fluid element in the capillary. According to Fick's law (6), the time needed for heat dissipation is directly proportional to the second power of the channel depth for a flat rectangular channel, assuming that the thermostated copper blocks and chip represent an infinite heat capacity relative to the heated fluid element (see Fig. 1B for instrument layout). Simple calculations have demonstrated that, in our micromachined device, heating and cooling times are each less than 100 ms.

The flow-through PCR system is based on a single channel passing repetitively through the three temperature zones (Fig. 1). The pattern of the chip layout determines the relative time a fluid element is exposed to each temperature zone. Moreover, the pattern defines the number of cycles  $n$  performed per run through the chip; the theoretical DNA amplification factor is thus  $2^n$ . We used a chip that generates 20 identical cycles, each having a time ratio of 4:4:9 (melting:annealing:extension), for a theoretical amplification factor of  $2^{20}$  (Fig. 1B); the first cycle contained a threefold extended melting time to ensure proper accessibility of the template DNA. Two of the three inlets of the chip were used for the continuous buffer flow and the sample injection (the third inlet was not used in these experiments). All fluids were pumped by hydrostatic pressure; the channel dimensions (40  $\mu\text{m}$  by 90  $\mu\text{m}$  by 2.2 m) were such that a pressure drop of 1 bar over the whole chip resulted in a flow-through time of 4 min for the 20 cycles.

**Fig. 2. (A)** PCR products by flow-through thermal cycling. All PCR reactions were performed with the same PCR mixture: 10 mM tricine (pH 8.4), 0.01% (w/v) Tween 20, 50 mM KCl, 0.2 mM deoxynucleotide triphosphate, 1.5 mM  $\text{MgCl}_2$ , 1.4  $\mu\text{M}$  polyvinylpyrrolidone, 1  $\mu\text{M}$  primers (5'-TGCACCGGC-GCGTACTGTA-3', 5'-CATCACATAACGCATAGC-3'), Taq (0.25 U/ $\mu\text{l}$ ), and  $\sim 10^5$  copies of template. Lane 1: Reference PCR performed in a very rapid commercial thermocycler (Hybaid, PCR Express) with a cycling time of 50 min for 20 cycles. Lanes 2 to 8: Flow-through PCR with increasing flow rates, 5.8 to 72.9 nl/s, corresponding to cycling times of 18.8 to 1.5 min for 20 cycles. Lane 9: negative control; PCR mixture without template run at a flow rate of 15.6 nl/s (as in lane 4) just after a run with normal template concentration. The rightmost lane is a 100-bp DNA ladder (15628-019, Gibco BRL). **(B)** Fluorescence was integrated over the indicated areas in (A) with ImageQuant software. Values were normalized to the fluorescence of the product from the reference cyclers (100%) and plotted against their total cycling time, that is, the time needed for a fluid element to pass through the 20 cycles of the chip. Because on each run 10  $\mu\text{l}$  had been collected for slab-gel analysis, the overall run time increased by the time needed to accumulate this large volume. Numbers correspond to the lanes in (A). A logarithmic regression was fitted to the data points.

The channel walls in the chip were silanized with dichlorodimethylsilane to reduce adsorption of enzyme and DNA to the glass surface; a zwitterionic buffer and a non-ionic surfactant were used as the PCR buffer to impart a dynamic coating (7). Primers were used that defined a 176-base pair (bp) product from the quinolone resistance-determining region of the *Neisseria gonorrhoeae* DNA gyrase gene (*gyrA*); the template used was a 1-kbp PCR fragment from the same gene. The chip was run with flow rates ranging from 5.8 to 72.9 nl/s, which represents a total flow-through time of 18.7 to 1.5 min for 20 cycles. For each amplification, 10  $\mu\text{l}$  of PCR mixture was injected and collected at the outlet of the chip for analysis. As a reference, the PCR mixture (10  $\mu\text{l}$ ) was run on a fast commercial thermal cycler (Hybaid, PCR-Express) with an overall cycling time of 50 min for 20 cycles. The collected samples were analyzed by an 8% (29:1) polyacrylamide gel stained with ethidium bromide. Fluorescence was imaged by a charge-coupled-device camera and quantitatively analyzed with the ImageQuant software package (Fig. 2A).

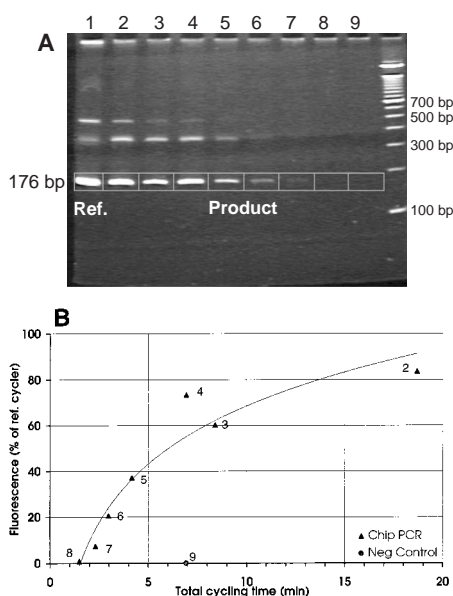
The results demonstrate that with a very simple device and virtually no optimization, PCR can be performed in continuous flow, yielding product quality and quantity comparable to standard thermal cycling methods (Fig. 2B). A negative control (Fig. 2A, lane 9), containing the whole PCR mixture except for the template, was run at a flow rate that should yield high amplification (for example, Fig. 2A, lane 4) subsequent to a sample run at high template concentration. No product could be detected, which is not sur-

prising because the location of high DNA concentration (the last few cycles of amplification) and the location of the first few critical amplification cycles were spatially separated. We suggest that cross-contamination in a continuous-flow format may be much less of a problem than in a stationary-tube PCR format. Thus, a flow-through PCR chip can be reused for extended periods without major cleaning. All runs in this study were done on the same chip by alternately injecting volumes of sample and buffer at a ratio of 1:0.8.

Very small samples can be run on the system. The only constraint is that the sample plug must be large enough for accurate injection into the channel, and this can be accomplished with sample plug volumes on the order of a few nanoliters. Because multiple sample plugs can travel at the same speed through the same chip, the potential throughput of a single device can be greatly increased.

To build a complex system analogous to an electronic integrated circuit, it is necessary to integrate a variety of other continuously working parts. A cursory glance at developments in miniaturized total analysis systems ( $\mu\text{TAS}$ ) during the past 5 years reveals that most of the relevant components, such as continuous-flow mixers (8), continuous-flow microreactors (9), continuous separations (10), and high-speed capillary gel electrophoresis (as a conventional batch process), have already been presented (11). Accordingly, the continuous-flow microamplifier should allow the creation of highly elaborate analysis and synthesis systems.

Although chemical amplification reactors will obviously not be applicable to all reactions, neither will they be limited to PCR. Devices of this kind open up whole new areas of application in medical diagnostics. For example, the online amplification and monitoring of a specific gene could show the patient's ability to metabolize a given drug so as to determine the ideal course of therapy. On-site analysis of patient samples could demonstrate the presence of bacterial DNA and any susceptibility to antibiotic treatment.



## REFERENCES AND NOTES

1. K. B. Mullis, F. Ferré, R. A. Gibbs, *The Polymerase Chain Reaction* (Birkhäuser, Boston, 1994).
2. H. Swerdlow, K. Dew-Jager, R. F. Gesteland, *Bio-techniques* **15**, 512 (1993).
3. J. Cheng, M. A. Shoffner, K. R. Mitchelson, L. J. Kricka, P. Wilding, *J. Chromatogr. A* **732**, 151 (1996).
4. A. T. Woolley *et al.*, *Anal. Chem.* **68**, 4081 (1996).
5. A. Manz and H. Becker, Eds., *Microsystem Technology in Chemistry and Life Sciences*, vol. 194 of *Topics in Current Chemistry* (Springer, Berlin, 1998).
6. E. L. Cussler, *Diffusion Mass Transfer in Fluid Systems* (Cambridge Univ. Press, Cambridge, 1984).
7. N. Chiem and D. J. Harrison, *Anal. Chem.* **69**, 373 (1997).

8. U. D. Larsen, J. Branerberg, G. Blankenstein, in *Proceedings of the 2nd International Symposium on Miniaturized Total Analysis Systems  $\mu$ TAS '96* (Analytical Methods & Instrumentation, Base 1, 1996), pp. 228–230.
9. T. Laurell and J. Drott, *Biosens. Bioelectronics* **10**, 289 (1995).
10. D. E. Raymond, A. Manz, H. M. Widmer, *Anal. Chem.* **66**, 2858 (1994).
11. C. S. Effenhauser, A. Paulus, A. Manz, H. M. Widmer, *ibid.*, p. 2949.
12. Supported by SmithKline Beecham, Zeneca, and a grant from the Biotechnology and Biological Sciences Research Council (UK). We thank B. Robertson, for primers and templates used in this study, and A. Ivens. We also thank Hybaid for the loan of their PCR instrument and the Alberta Micro-electronic Centre for the production of the microchips.

15 December 1997; accepted 23 March 1998

## Predatory Dinosaur Remains from Madagascar: Implications for the Cretaceous Biogeography of Gondwana

Scott D. Sampson,\* Lawrence M. Witmer, Catherine A. Forster, David W. Krause, Patrick M. O'Connor, Peter Dodson, Florent Ravoavy

Recent discoveries of fossil vertebrates from the Late Cretaceous of Madagascar include several specimens of a large theropod dinosaur. One specimen includes a nearly complete and exquisitely preserved skull with thickened pneumatic nasals, a median frontal horn, and a dorsal projection on the parietals. The new materials are assigned to the enigmatic theropod group Abelisauridae on the basis of a number of unique features. Fossil remains attributable to abelisaurids are restricted to three Gondwanan landmasses: South America, Madagascar, and the Indian subcontinent. This distribution is consistent with a revised paleogeographic reconstruction that posits prolonged links between these landmasses (via Antarctica), perhaps until late in the Late Cretaceous.

Dinosaurs underwent their greatest diversification during the Late Jurassic and Cretaceous. Although plate tectonics during this interval had a profound impact on the evolution of dinosaurs and coeval terrestrial faunas, this impact remains poorly understood, in part because of a paucity of fossil remains from southern continents. Recent expeditions have resulted in important dinosaurian discoveries on all major landmasses that once formed the southern supercontinent of Gondwana, and it is now possible to begin assessing the biogeographic history of dinosaurian clades, at least on a gross scale (1, 2).

Current models of the sequence and timing of Gondwanan fragmentation are based predominantly on geophysical evidence and have yet to be rigorously tested with non-

marine fossils. Plate fragmentation can set minimum dates for the origin of particular terrestrial and freshwater clades if members are present on two or more landmasses. Conversely, phylogenetic patterns can provide increased paleogeographic resolution and serve as independent tests of tectonic models (3).

Here, we describe theropod dinosaur fossils from the Upper Cretaceous (?Campanian) Maevarano Formation, Mahajanga Basin, northwestern Madagascar (4). Fragmentary dinosaur remains have been reported from the Mahajanga Basin for more than a century (5), with three taxa erected during that period (5–7): a sauropod, *Titanosaurus madagascariensis*; a theropod, *Majungasaurus crenatissimus*; and a pachycephalosaur, *Majungatholus atopus*. Recent excavations in this same field area have yielded a rich diversity of fossil vertebrates, including abelisaurid theropods, titanosaurid sauropods, birds, crocodylians, snakes, turtles, fishes, frogs, and mammals (8–10). The fossils occur predominantly in coarse-grained sandstone facies, and a variety of indicators suggest a semi-arid, seasonal depositional environment (11). Many specimens occur as disarticulated yet associated skeletons amassed into concentrations, likely representative of time-averaged assemblages (11).

One of the theropod specimens (FMNH PR 2100) includes a nearly complete skull

(12)—among the best preserved and most complete dinosaur skulls known—and most of the tail. The skull is disarticulated and individual bones are virtually undistorted, allowing comprehensive and detailed study of all elements (Fig. 1). The external surface of many elements is covered in rugose sculpturing, and the skull roof is adorned with three median ornamentations: thickened, fused nasals; a low frontal horn; and a parietal eminence. The total skull length is 57 cm, and comparisons with a closely related taxon, *Carnotaurus sastrei* from Argentina (13), suggest a total adult body length of about 7 to 9 m. A second specimen (UA 8678) of the same taxon includes an incomplete and disarticulated skull, most of the precaudal axial column, and the left ilium. Several of the vertebrae and ribs, particularly in the cervical region, were recovered in articulation. The small size of the skull elements relative to those of FMNH PR 2100, combined with the lack of fusion between several vertebral centra and corresponding neural arches, indicates that this animal was immature at the time of death.

Although large theropod materials from the Maevarano Formation have generally been referred to *Majungasaurus crenatissimus* (5, 6, 9), the inadequacy of the holotype and neotype specimens (14) requires that this taxon be regarded as a *nomen dubium*. Comparison of the recently collected materials with the fragmentary holotype specimen of the putative Malagasy pachycephalosaur, *Majungatholus atopus*, demonstrates that *Majungatholus* is not a pachycephalosaur but rather a “domed” theropod (15). This finding has biogeographic significance in that it removes the only report of a pachycephalosaur from a Gondwanan landmass, thereby restricting occurrences of this dome-headed ornithischian clade to Laurasia. Thus, the materials described herein are referred to *Majungatholus atopus* and placed within the enigmatic theropod group Abelisauridae (16).

The skull of *Majungatholus atopus* is relatively short and broad, with large antorbital, laterotemporal, and external mandibular fenestrae (Fig. 1). The snout is blunt and relatively deep at the level of the nares, with elongate, thickened, and rugose nasals. A large, bilateral pneumatic foramen pierces the fused nasals, and computerized tomographic (CT) imaging demonstrates that this structure is virtually hollow, supported internally only by thin bony struts. The orbital fenestra is rounded dorsally, with processes of both the lacrimal and postorbital projecting into it ventrally, outlining the position of the eye. Just caudal to the nasals is a roughened, conical median projection arising from the frontals. CT imaging shows this frontal horn to be hollow as well. The holotype of

S. D. Sampson, Department of Anatomy, New York College of Osteopathic Medicine of New York Institute of Technology, Old Westbury, NY 11568, USA.

L. M. Witmer, Department of Biomedical Sciences, College of Osteopathic Medicine, Ohio University, Athens, OH 45701, USA.

C. A. Forster, D. W. Krause, P. M. O'Connor, Department of Anatomical Sciences, State University of New York, Stony Brook, NY 11794, USA.

P. Dodson, Laboratories of Anatomy, Department of Animal Biology, School of Veterinary Medicine, University of Pennsylvania, Philadelphia, PA 19104, USA.

F. Ravoavy, Université d'Antananarivo, Service de Paléontologie, Antananarivo (101), Madagascar.

\*To whom correspondence should be addressed: E-mail: ssampson@iris.nyit.edu